Invited Paper

Experimental and Theoretical demonstration of noise shaping by interspike interval correlations

Maurice J. Chacron[a], Benjamin Lindner[b], Leonard Maler[c], André Longtin[b,c], and Joseph Bastian[a]

[a] Department of Zoology, University of Oklahoma, 730 van vleet Oval, Norman, Oklahoma, USA;
[b] Department of Physics, University of Ottawa, 150 Louis Pasteur, Ottawa, Ontario, Canada
[c] Department of Cellular and Molecular Medicine, University of Ottawa, 451 Smyth rd., Ottawa, Ontario, Canada

ABSTRACT

Neurons often display complex patterns of action potential firing in response to a wide variety of inputs. Correlations amongst the interspike interval sequence are often seen in experimental data from sensory neurons including electroreceptor afferents from weakly electric fish. Here we review some of our recent computational, theoretical, and experimental results on the mechanism by which negative interspike interval correlations increase information transfer: noise shaping. This mechanism might explain the behavioral hypersensitivity displayed by weakly electric fish when detecting prey.

Keywords: Noise Shaping, Information Transfer, neuron, weakly electric fish, correlations

1. INTRODUCTION

Understanding the neural code (i.e. how information is encoded by sensory neurons and then later decoded by the brain) remains a largely unsolved problem in neuroscience.[1] Neurons are not deterministic: the same stimulus, when repeatedly presented, will give rise to different output spike trains.[2] This is mostly due to the fact that neurons have to operate in the presence of a significant amount of noise. Noise can come from two main sources: external and internal. External noise sources come from the environment itself. One famous example is the cocktail party problem where one listens to a particular speaker over background chatter.[3] Internal noise sources can come from the random opening and closing of voltage-gated ion channels: so-called flicker noise.[4] They can also come from the intense synaptic bombardment that exists under in vivo conditions.[5]

There are two main points of view regarding the way by which sensory systems deal with noise. Noise can be used to enhance information transfer about relevant stimuli through stochastic resonance[6,7] where the output signal-to-noise ratio displays a maximum as a function of the noise intensity. Stochastic resonance is exclusively seen in the subthreshold regime at the single neuron level (i.e. the stimulus by itself is insufficient to generate action potentials). On the other hand, if a single neuron operates in the suprathreshold regime, the signal-to-noise ratio then decreases monotonically as a function of noise intensity with the exception of suprathreshold stochastic resonance which only occurs in a neural population.[8] From this point of view, noise is unwanted and must be minimized in order to improve information transmission.

Many electronic devices such as Sigma-Delta modulators[9] and Josephson junctions[10,11] must operate in the presence of noise. This operation is facilitated through a phenomenon called noise shaping: noise power is shifted from one frequency range to another thereby improving signal transmission in the former frequency range and

Further author information: (Send correspondence to M.J.C.)
M.J.C: E-mail: mauricejchacron@yahoo.ca, Telephone: 1 405 325 5271
B.L.: E-mail: benjamin.lindner@science.uottawa.ca, Telephone: 1 613 562 5800 6744
L.M.: E-mail: lmaler@uottawa.ca, Telephone: 1 613 562 5800 8189
A.L.: E-mail: alongtin@science.uottawa.ca, Telephone: 1 613 562 5800 6762
J.B.: E-mail: jbastian@ou.edu, Telephone: 1 405 325 5271

Fluctuations and Noise in Biological, Biophysical, and Biomedical Systems III, edited by Nigel G. Stocks, Derek Abbott, Robert P. Morse, Proc. of SPIE Vol. 5841 (SPIE, Bellingham, WA, 2005) · 0277-786X/05/$15 · doi: 10.1117/12.610938

worsening it in the latter. It has been proposed that the brain might use noise shaping as a mechanism to deal with noise[12,13] and a modeling study has shown that noise shaping could result from inhibitory coupling in a neural network.[14]

Neurons both at the periphery and in the cortex can show correlations amongst successive interspike intervals,[15–20] making them non-renewal processes.[21] This indicates that memory is carried from one action potential to the next and is not "erased" as in a renewal process. This adds an extra complication in the calculation of mean first passage time moments and the spike train power spectrum.[22–24]

In this paper, we review some of our recent theoretical and experimental results showing that ISI correlations lead to noise shaping of the resulting spike train which enhances information transmission and moreover that weakly electric fish may use this strategy to maximize their capabilities of detecting prey. The paper is organized as follows: first, weakly electric fish and the low-frequency characteristics of prey stimuli are introduced in section 2. Experimental data from electroreceptor afferents showing ISI correlations are then shown and we review modeling results showing that negative ISI correlations can enhance information transfer in section 3. In section 4, we introduce simplified models where theoretical calculations are possible and show analytically and through numerical simulations that noise shaping by negative ISI correlations can enhance information transmission of low frequency stimuli. Section 5 shows that noise shaping is indeed present in experimental data from electroreceptor afferents and we predict the net information gain brought about by this noise shaping.

2. ELECTRORECEPTOR AFFERENTS FROM WEAKLY ELECTRIC FISH

Weakly electric fish use distortions of their self-generated electric field, the electric organ discharge (EOD), in order to detect prey and communicate with conspecifics.[25] Prey signals from zooplankton (Daphnia) are faint, spatially localized, and typically contain temporal frequencies below 30 Hz.[26] However, communication signals from conspecifics and spatially diffuse and typically contain frequencies above 50 Hz.[27] Electroreceptor afferents on their skin detect amplitude and phase modulations of the EOD and transmit this information through trains of action potentials.[28,29] We will concentrate on the amplitude coding or P-type electroreceptors here. These increase their firing rates in response to increases in EOD amplitude[28,30] and display significant adaptation.[30–32] Moreover, they show baseline activity (i.e. in the presence of the unmodulated EOD) with high firing rates.[28,30] Closer inspection of this activity has shown that short interspike intervals followed longer ones preferentially and vice-versa: leading to negative ISI correlations.[18–20] This is shown in figure 1. Figure 1A shows an intracellular recording from the afferents' axon and already it can be seen that long interspike intervals follow short ones and vice-versa. Figure 1B shows the multimodal ISI distribution that results from phase locking to the quasi-sinusoidal EOD.[20,30] Figure 1C shows the ISI serial correlation coefficients (SCC) ρ_j defined by:

$$\rho_j = \frac{\langle (I_{i+j} - \langle I_i \rangle)\,(I_i - \langle I_i \rangle) \rangle}{\langle (I_i - \langle I_i \rangle)^2 \rangle} \tag{1}$$

where $\{I_i\}$ denotes the ISI sequence, j is the lag, and the average $< ... >$ is performed over index i. A strong negative SCC is seen at lag one. It was shown that the EOD phase locking alone was not sufficient to account for these strong negative ISI correlations.[20] Although there is considerable heterogeneity in the electroreceptor afferent population particularly in their ability to produce packets of action potentials,[30,31] all units seen so far have shown ISI correlations to some degree although in some of the more bursty units show SCCs that alternate in sign and decay over a few lags. Similar temporal anti-correlations have also been observed in paddlefish electroreceptors.[33,34]

3. MODELING ELECTRORECEPTOR AFFERENTS

The leaky integrate-and-fire neuron is perhaps one of the simplest neuron models.[35] In this model, the membrane voltage v obeys the dynamics of an RC circuit. The nonlinearity of the action potential genesis is captured by the following reset rule: once v reaches a constant threshold value w, it is reset to a value v_{reset} and an action potential is said to have occurred. While it is capable of reproducing a variety of experimental results such as the all-or-none nature of the action potential and phase locking to sinusoidal input, the leaky integrate-and-fire model generates renewal spike trains in the presence of Gaussian white noise[36] or sinusoidal input.[37,38] It must thus be modified to include a variable that will carry the memory from one action potential to the next.

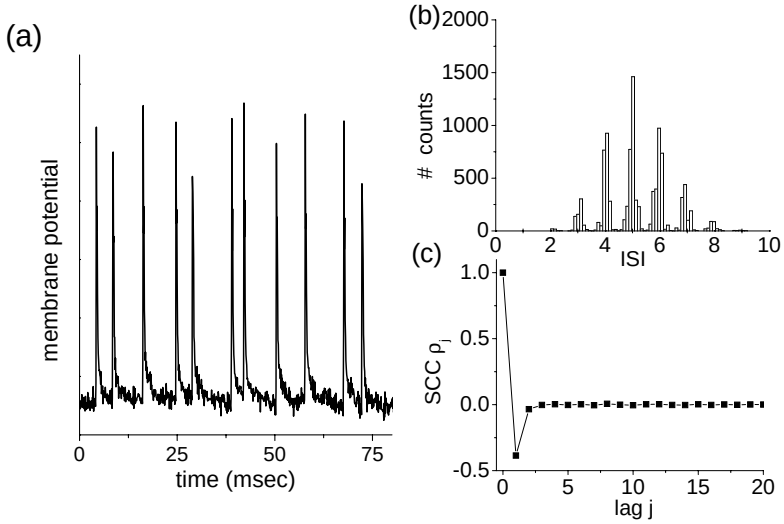

Figure 1. (a) Intracellular recording from a receptor afferent. Patterning in the ISI sequence is seen in that long ISIs tend to follow short ones. (b) ISI distribution from the data. Multiple modes are seen as receptor afferents are phase-locked to the animal's quasi-sinusoidal EOD. (c) ISI SCC's ρ_j as a function of lag j. We have $\rho_1 < 0$ indicating that afferent spike train is a non-renewal process.

3.1. Model Description

An ideal variable for this is the action potential threshold w. Previous models have incorporated random time varying thresholds[39, 40] and recent experimental data has shown that the action potential threshold was variable in vivo.[41] We thus made the threshold w vary in time as well. We termed this addition to the LIF model the leaky integrate-and-fire with dynamic threshold (LIFDT) model[20, 42–48] and it is described by the following differential equations:

$$\dot{v} = -\frac{v}{\tau_v} + I_{syn} \tag{2}$$

$$\dot{w} = H(t - t_{last} - T_r)\left(\frac{w_0 - w}{\tau_w}\right) + \Delta w\,\delta(t - t_{last}) \tag{3}$$

$$I_{syn} = [A_0 + A(t)]H[A_0 + A(t)]\sin[2\pi f_{EOD}\,t]\,H[\sin(2\pi f_{EOD}\,t)]\,[1 + \xi(t)] \tag{4}$$

where v is the membrane voltage, w is the threshold, T_r is the absolute refractory period, t_{last} is the last spiking time, and I_{syn} is the synaptic current, A_0 is the baseline EOD amplitude, $A(t)$ is the amplitude modulation, and f_{EOD} is the EOD frequency. $\xi(t)$ is Gaussian white noise of zero mean. $H(.)$ is the Heaviside function ($H(x) = 1$ if $x >= 0$ and $H = 0$ otherwise) and accounts for synaptic rectification.[20] We let the threshold carry the memory by the following firing rule: when $v = w$, v is reset to $v_{reset} = 0$ as in a standard LIF model, while threshold is incremented by a constant amount Δw and kept constant for the duration of the absolute refractory period T_r; after this time T, the threshold relaxes exponentially towards its equilibrium value w_0 until the next spiking time. If two spiking times occur within close proximity of one another, the threshold will cumulatively increase leading to greater refractoriness. Thus, a short ISI will tend to be followed by a long one and the model displays negative ISI correlations[44] as in the experimental data from the electroreceptor neuron.[20]

3.2. Modeling results

Figure 2A shows a time series from the model under baseline activity (i.e. $A(t) = 0$). It is seen that a short ISI causes a cumulative increase in the threshold variable w. The longer time needed for w to decay will cause the next ISI to be longer. We note that this is a deterministic property of the model[44] and that the noise $\xi(t)$ constantly perturbs the system away from its stable periodic firing pattern observed deterministically, thus

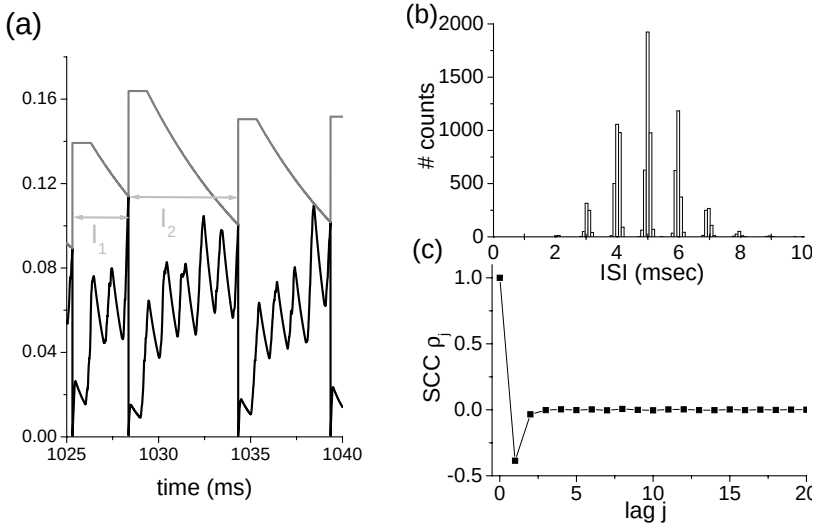

Figure 2. (a) Time series showing the voltage v (black) and threshold w (grey) from the LIFDT model. A short ISI such as I_1 causes accumulation in the threshold w which will thus rise to a higher value. Consequently, the next ISI I_2 will be longer. (b) ISI distribution from the LIFDT model's under baseline activity(i.e. $A(t) = 0$). (c) ISI SCC's from the model showing $\rho_1 < 0$ as in the experimental data. Overall, good agreement is seen with the experimental data. Parameter values were previously given.[20]

causing the negative ISI correlations. The ISI distribution from the LIFDT model is shown in figure 2B while figure 2C shows the SCCs from the model. Close agreement is observed with the experimental data and different values for the parameters in the model as well as a minor addition to produce bursting dynamics can reproduce the heterogeneities seen experimentally.[23, 42, 48]

In order to quantify the effects of ISI correlations on information transmission, we compared the output of the LIFDT model to that of a previous model proposed for electroreceptor afferents.[43] This previous model has been proposed to describe electroreceptor afferent dynamics.[49] However, we found that spike trains produced by that model lacked the negative ISI correlations that were so prominent in the data.[43] These models were thus an ideal tool to study the effects of ISI correlations as the first order ISI statistics of the two models were virtually identical. Low-passed filtered Gaussian white noise input with cutoff frequency f_c and variance $\sigma^2 = 2\alpha f_c$ was given to both models and information theory[50, 51] was used to compute the rate of information transmission of both models. Figure 3A shows the mutual information rate from both the Nelson and LIFDT models as a function of stimulus standard deviation σ while figure 3B shows the mutual information rates as a function of cutoff frequency f_c.[43] It is seen that the LIFDT model has a higher rate of information transmission than the Nelson model over a wide range of stimulus intensities and frequency content. The gain in information can be as high as 50%. Similar results were obtained with signal detection measures.[43, 45] However, little insight as to the actual mechanism by which these correlations increase information transmission can be ascertained from these numerical simulations. In the next section, we develop more abstract models from which analytical results can be obtained and the mechanism revealed.

4. THE MECHANISM: NOISE SHAPING

4.1. Two simple integrate-and-fire models

In order to understand the effect of ISI correlations on information transmission, we need models that will capture the essence of the phenomenon without extraneous parameters. We thus constructed two simple perfect integrate-and-fire neuron models which will be henceforth referred to as models A and B.[23, 24]

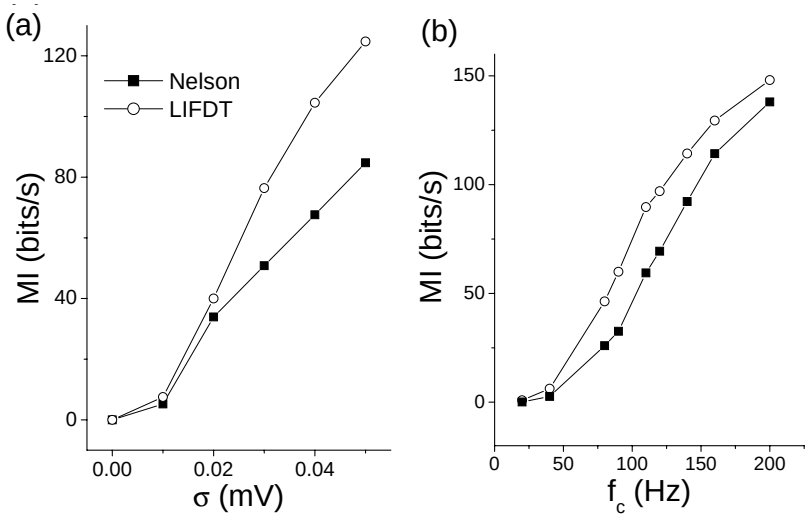

Figure 3. (a): Mutual information rates for the LIFDT and Nelson models as a function of σ and $f_c = 100$ Hz. (b): Mutual information rates as a function of cutoff frequency f_c for $\sigma = 0.03$ mV. The LIFDT model consistently gives greater information rates than the Nelson model. Parameter values were previously given.[43]

For both models, the input is integrated without leakage according to:

$$\dot{v}(t) = \mu + s(t) \tag{5}$$

where μ is a constant base current and $s(t)$ is the input signal to be transmitted. We do not include the internal noise of the neuron as a fluctuating input current but choose the mathematically simpler construction of noisy threshold and reset points. As previously mentioned, we note that there is also some experimental evidence for a fluctuating threshold.[41,52]

The models differ in their reset rules for the voltage v. A time series for the voltage and threshold of model A is illustrated in figure 4A. The threshold $\theta(t)$ is constant between spikes and is drawn from a uniform distribution in the interval $[\Theta_0 - D, \Theta_0 + D]$ with Θ_0 being the mean threshold and D standing for the noise intensity. We assume a small value $D < \Theta_0/2$. When $v(t) > \theta(t)$, a spike is fired, a new threshold is drawn, and the voltage is decremented by Θ_0, i.e. $v \to v - \Theta_0$. It is easily seen that the voltage reset value will be uniformly distributed in the interval $[-D, D]$. However, this reset rule correlates a given threshold value with the subsequent voltage reset value and, as we shall see, this gives rise to a strong ISI SCC at lag one in the absence of stimulation (i.e. $s(t) = 0$).

A time series for the voltage and threshold of model B is illustrated in figure 4B. The threshold $\theta(t)$ is still constant between spikes and is drawn from a uniform distribution in the interval $[\Theta_0 - D, \Theta_0 + D]$. However, the reset value for the voltage v is now drawn randomly from a uniform distribution in the interval $[-D, D]$. There will thus be no correlation between a given threshold value and the subsequent voltage reset value. Model B will thus not generate any non-zero ISI SCCs at lags> 0.

We now calculate the ISI SCCs of both models. We see from Fig. 4A that an ISI I_j can be split up into two contributions $I_j = u_j + v_j$ where u_j and v_j are the passage times from the reset point to half of the mean threshold $(\Theta_0/2)$ and from $\Theta_0/2$ to the random threshold $\Theta(t)$. Due to the correlation between the random threshold and the subsequent reset value in model A, we have

$$v_j + u_{j+1} = \frac{\Theta_0}{\mu} \tag{6}$$

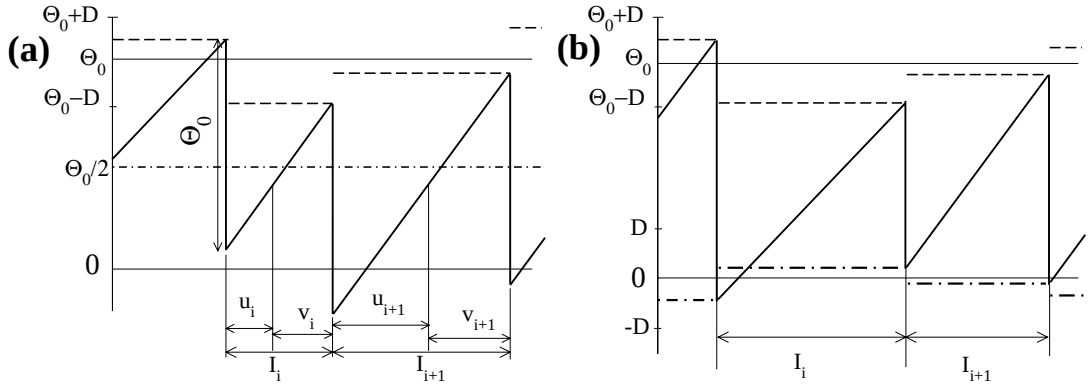

Figure 4. Illustration of simplified models. (a): Model A for $s(t) \equiv 0$. In between action potentials the voltage $v(t)$ (solid line) evolves according to eq. 5. A threshold value (shown by the dashed line) has been drawn from the uniform density $[\Theta_0 - D, \Theta_0 + D]$ the boundaries of which are indicated. Once the voltage hits the threshold, a spike is fired and v is decremented by Θ_0. Each ISI I_j consists of two sub-intervals u_j and v_j that are defined as the passage times from reset to $\Theta_0/2$ (dotted line) and from the latter point to the threshold, respectively. (b): Model B for $s(t) \equiv 0$. In this case, threshold values (dashed line) and reset values are drawn from uniform densities the boundaries of which are indicated. Note that both random values (drawn after each firing) are independent of each other in marked contrast to model A. A subdivision of the indicated intervals as for model A is also possible but has here been omitted for the sake of clarity of the illustration.

We can use this to calculate the covariance between subsequent ISIs at lag one:

$$\langle I_j I_{j+1} \rangle - \langle I_j \rangle^2 = -\frac{1}{2}(\langle I_j^2 \rangle - \langle I_j \rangle^2) \tag{7}$$

As a consequence, we obtain for the SCCs of model A $\rho_i^A = \delta_{0,i} - \frac{1}{2}\delta_{1,i}$ with $\delta_{1,i}$ being the Kronecker symbol. A similar calculation for model B gives $\rho_i^B = \delta_{0,i}$.

Models A and B furthermore generate ISIs with an identical density[22,24] which facilitates their comparison. Since both u_j and v_j are uniformly distributed in the intervals $[(\Theta_0/2 - D)/\mu, \Theta_0/2 + D)/\mu]$, this ISI density is then given by the convolution of these two random variables which yields a triangular distribution.

4.2. Calculation of the power spectrum of baseline activity

We used the following formula to compute the power spectra of models A and B[52]:

$$S(f) = \frac{1}{\langle I \rangle}\left[1 + \sum_{n=1}^{\infty} F_n(f) + F_n(-f)\right] \tag{8}$$

where $F_n(s)$ is the Fourier transform of the nth order interval density. A straightforward calculation gives[22,24]:

$$P_{A0}(f) = \frac{1}{\langle I \rangle}\left[1 - \frac{\sin^2(\beta f)}{(\beta f)^2}\left(1 - \frac{1}{\langle I \rangle}\sum_{n=-\infty}^{\infty}\delta(f - \frac{n}{T})\right)\right] \tag{9}$$

and

$$P_{B0}(f) = \frac{[(\beta f)^4 - \sin^4(\beta f)]/\langle I \rangle}{(\beta f)^4 - 2(\beta f)^2 \sin^2(\beta f)\cos(2\pi\langle I \rangle f) + \sin^4(\beta f)} \tag{10}$$

where $\beta = 2\pi D/\mu$ and the mean ISI is given by $\langle I \rangle = \Theta_0/\mu$.

The power spectra of models A and B are shown in figure 5A. At low frequencies ($f < 0.25$) and also in the range around the mean firing rate of the neuron ($f \approx 1$), the spectrum of model A shows much less power

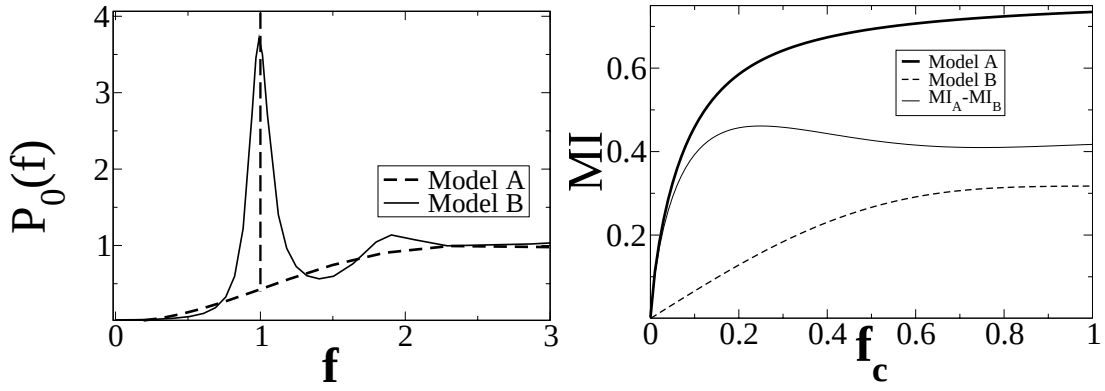

Figure 5. *Left*: Power spectra for the spike trains of the simplified models and $s(t) \equiv 0$. *Right*: Mutual information for models A and B (solid and dashed lines) vs cutoff frequency f_c ($\alpha = 0.0156$); also shown is the difference between these functions (thin solid line).

(except, of course, for the δ peak at $f = 1$) than the spectrum of model B. The noise power lacking in this range is, however, exactly compensated by an excess in other frequency ranges and by the power contained in the δ peaks. This is because the integral over the spectrum equals the inverse Fourier transform at vanishing argument, i.e. according to the Wiener-Khinchine theorem the spike train's correlation function at zero lag. At arbitrary lag we have:

$$\begin{aligned} \int_{-\infty}^{\infty} df e^{-2\pi i f \tau} \frac{S(f) - r_0}{2\pi} &= \langle \tilde{x}(t)\tilde{x}(t+\tau)] \rangle - r_0 \delta(\tau) \\ &= r_0(m(\tau) - r_0) \end{aligned} \tag{11}$$

Here $m(\tau)$ is the probability per unit time to observe a spike under the condition that at $\tau = 0$ a spike has occurred and r_0 is the baseline firing rate which is identical for both models as they have equal ISI density functions. Note that this does not include the reference spike but any other (not only the first occurring after the reference spike). Since both models A and B show an absolute refractory period, we have $m(0) = 0$. At zero lag, the l.h.s. is proportional to the integrated power considered above, while the r.h.s. approaches $-r_0^2$ for both models A and B. We thus have a shaping of the baseline spectrum by the negative ISI correlations. As will be seen later, the baseline spectrum is considered to be a noise spectrum of the system because the baseline activity is uncorrelated with $s(t)$.

This noise shaping increases the available information that can be transmitted about a time varying signal $s(t)$. Figure 5B shows the mutual information density curves for both models as a function of stimulus cutoff frequency f_c. The mutual information rate for model A is always larger than the mutual information rate of model B.

4.3. Using linear response theory to predict the response to time varying input

We used linear response theory[53] to compute the response of both models A and B to a time varying signal $s(t)$. The spike train in response to $s(t)$ is then given by in the Fourier domain:

$$\tilde{X}(f) = \tilde{X}_0(f) + \chi(f)\tilde{s}(f) \tag{12}$$

where $\chi(f)$ is the susceptibility function. It turns out that it is identical for both models A and B[22,24] and is given by:

$$\chi_A(f) = \chi_B(f) = r_0/\mu \tag{13}$$

The mutual information rate (in bits/sec) is given by[1]:

$$MI = -\int_0^{f_c} df \log_2[1 - C(f)] \tag{14}$$

$$C(f) = \frac{|X(f)|^2}{P(f)S_{st}(f)} \tag{15}$$

where $C(f)$ is the coherence function, $X(f) \equiv < \tilde{X}^*(f)\tilde{s}(f) >$ is the cross-spectrum between the spike train $X(t)$ and the signal $s(t)$, $P(f) \equiv < \tilde{X}^*(f)\tilde{X}(f) >$ is the spike train power spectrum, and $S_{st}(f) \equiv < \tilde{s}(f)^*\tilde{s}(f) >$ is the signal power spectrum. Note that this formula is only valid if the signal $s(t)$ has a Gaussian probability distribution. The power spectrum in response to a signal $s(t)$ is given by:

$$P(f) = P_0(f) + |\chi(f)|^2 S_{st}(f) \tag{16}$$

Using equations (12), (13-16), we get the following expression for the mutual information rate of models A and B:

$$MI_{A,B} = \int_0^{f_c} df \log_2 [1 + SNR_{A,B}(f)] \tag{17}$$

$$SNR_{A,B}(f) = \frac{\theta_0^{-1} S_{st}(f)}{P_{A0,B0}(f)} \tag{18}$$

where $SNR_{A,B}(f)$ is the output signal-to-noise ratio of both models[1] and $P_{A0}(f)$,$P_{B0}(f)$ are given by equations (9) and (10), respectively. We note that the difference between models A and B only appears through the baseline power spectrum. Equation (18) furthermore explicitly shows the role of the baseline spectrum as a noise spectrum in both models.

We note that the linear response ansatz works well at large internal noise intensity ($D > 0.1$) but fails in the weak noise limit as can be expected. A more elaborate theory in the latter case has been developed.[24]

The mutual information rates of both models are shown in figure 5B. The shaping of the baseline spectrum leads to a lower power at low frequencies. This noise shaping gives rise to a higher output signal-to-noise ratio and thus a higher information rate for model A than for model B at these frequencies. The construction of models A and B have thus permitted us to understand the precise mechanism by which ISI correlations increase information transmission: noise shaping of the baseline power spectrum.

5. EXPERIMENTAL VERIFICATION OF NOISE SHAPING

Armed with the prediction from the theory, we now return to the original experimental data that inspired us to work on the problem. We thus recorded intracellularly from electroreceptor afferent axons in weakly electric fish. The experimental protocol was described previously in detail.[30, 54–56] Figure 6A shows the power spectrum (black) of one representative receptor afferent under baseline activity. The inset shows the ISI SCCs under the same conditions. As predicted by the theory, the baseline spike train power spectrum displays low power at low frequencies. We note that this is precisely the frequency range of behaviorally relevant prey stimuli (< 20 Hz). It is currently impossible to experimentally manipulate the system such as to remove the negative ISI correlations. However, we can randomly shuffle the ISI sequence in order to eliminate ISI correlations while keeping the same ISI distribution. The power spectrum of the resulting spike train in also shown (grey) in figure 6A and displays less structure. In particular, there is now more noise power at low frequencies. The inset shows that ISI correlations were indeed removed by this shuffling procedure.

Electroreceptor afferents were now stimulated by amplitude modulations of the animal's own EOD. The amplitude modulations signal used was low-pass filtered white noise with cutoff frequency $f_c = 120$ Hz. The typical contrast used (i.e. the standard deviation of the amplitude modulation signal to baseline EOD amplitude ratio) was 20%. Figure 7 shows the coherence curve (black) in response to the stimulus for that same electroreceptor

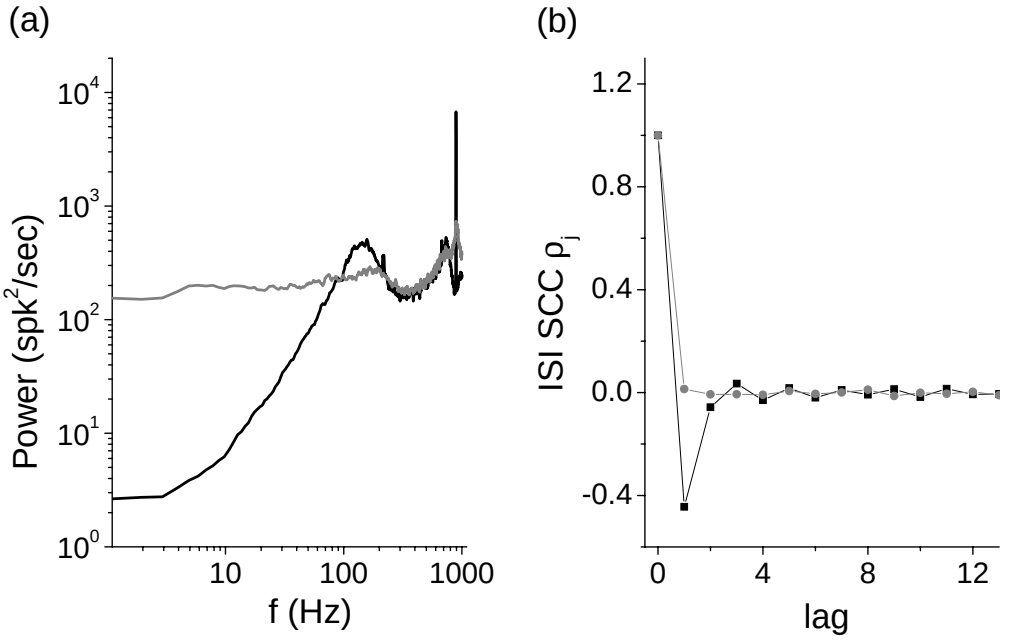

Figure 6. (a): Power spectrum of an experimentally obtained spike train from a receptor afferent under baseline activity (black). We randomly shuffled the ISI sequence and plotted the power spectrum of the resulting spike train (grey). This procedure eliminates ISI correlations and the spike train is now a renewal process. (b) ISI SCC's of the raw data (black squares) and the shuffled data (grey circles) showing that negative ISI correlations are indeed removed by the shuffling procedure.

afferent. The broadband response allows the electroreceptor population to respond equally well to both low frequency and high frequency stimuli.[56]

In order to quantify the gain in information brought about by ISI correlations in the data, we apply linear response theory to the experimental data. The theory is applied as follows. The spike train power spectrum in response to the input is given by equation (16. We computed the susceptibility from the cross-spectrum between the raw data spike train and the stimulus. From this, we can use equations (15) to compute the predicted coherence curve which is shown in grey in figure 7. The linear response theory overestimates the coherence, particularly for low frequency stimuli. This indicates that nonlinear effects are present. These will weaken the coherence by adding contributions to the power spectrum which are not captured in equation (16). Nevertheless, there is a qualitative agreement between the coherence of the raw data and the one predicted from linear response theory in that they both show a good response for low frequencies.

We also used the power spectrum of the shuffled spike train in equation (16) and computed the resulting coherence curve which is shown in light gray in figure 7. This would be the predicted coherence from a renewal process with the same ISI distribution as the raw data. It is seen that there is a net loss in information transmission and that this loss is greatest for frequencies below 20 Hz. Again, the linear response theory will lead to an overestimation of the coherence: the loss in low frequency coherence might be even greater. As such, it is most likely that noise shaping by ISI correlations is used by electroreceptor afferents and this may explain the hypersensitivity observed in weakly electric fish in detecting faint electrical signals from prey stimuli.[26]

6. DISCUSSION

We have reviewed some of our recent experimental and theoretical results pertaining as to the role of ISI correlations in information transmission. As beforementioned, these ISI correlations occur in a variety of sensory

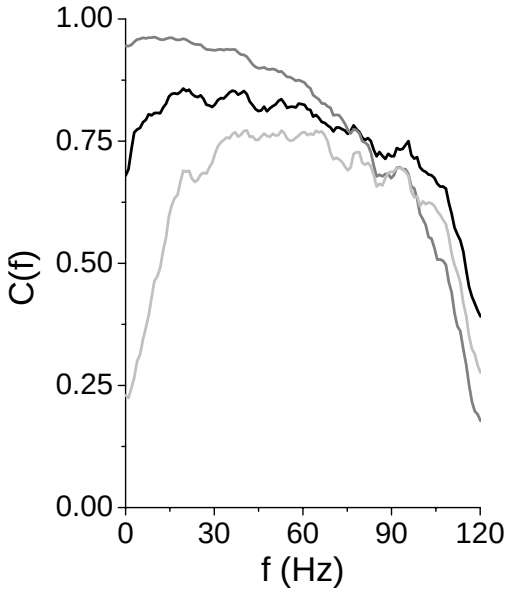

Figure 7. Coherence between the spike train and the stimulus for the raw data (black). Also shown is the coherence predicted by linear response theory (dark grey). There is an overestimation of the coherence for low frequencies but good qualitative agreement is seen since both curves have the same shape. We also used the power spectrum of the shuffled data to predict the coherence of a renewal process to input (light grey). Increasing the noise level at low frequencies results in a dramatic decrease in the coherence at these frequencies.

neurons at the periphery[15,16,33,34] as well as in the cortex.[17] The noise shaping strategy presented here could thus be occurring in other sensory modalities.

The exact biophysical cause of the negative ISI correlations in electroreceptor neurons is still unknown although there exists several hypothesis. Cumulative inactivation of sodium channels[57] could for example give rise to neural adaptation and ISI correlations. However, a fast spike activated slowly inactivating negative current could also give rise to similar effects: a likely candidate would be members of the KV family of potassium currents[58] that are present in electroreceptor afferents.[59] Another candidate could be a calcium activated potassium current such as I_{ahp}. This current was first shown to be present in cortical neurons[60] and was later discovered to be ubiquitous in the central nervous system. This current is also present in electroreceptors[61] and previous studies have shown that models incorporating such a current could display negative ISI correlations.[62,63] Furthemore, it was shown that such models were qualitatively equivalent to our LIFDT model.[63]

The presence of negative ISI correlations is linked with firing rate adaptation to step currents.[44,63] Electroreceptor afferents display strong adaptation properties.[30] Although our theoretical results only predicted that negative ISI correlations only increased information transmission of low-frequency stimuli. Our numerical simulations and the experimental data predict an increase for high frequencies as well.[43,56] A recent experimental study dealing with communication stimuli in weakly electric fish as shown that adaptation, and thus ISI correlation, in receptor afferents could help them discriminate communication signals.[32] Further theoretical work is necessary in order to understand this.

We note that long term positive ISI correlations have also been observed in several sensory neurons.[16,64] As might be expected, these increase neural variability and instead reduce the detectability of very low frequency stimuli. Sensory systems also use these to ignore long term trends in sensory stimuli.

Recent studies have shown that the post-synaptic targets of electroreceptor afferents, pyramidal cell, were

highly selective in their response to spatially diffuse communication stimuli.[65,66] Further studies have revealed that pyramidal cell properties were highly dependent on whether the stimulus was prey like, or communication like.[54,55,67,68] In particular, pyramidal cells were shown to be most sensitive to low frequency stimuli when the stimulus' spatial extent was prey-like, and to be most sensitive to high frequency stimuli when the stimulus' spatial extent was communication-like.[68] The relatively broadband tuning of electroreceptor afferents seen experimentally and brought about by negative ISI correlations would be ideal for this as filtering mechanisms would then allow pyramidal cells to extract behaviorally relevant information. In particular, the experimentally observed good response of pyramidal cells to low frequency stimuli indicates that they decode at least part of the information transmitted by electroreceptor afferents about these stimuli.[56,68]

Finally, although the inspiration for this work was biology, we note that the need for reducing low frequency noise is not constrained to biology only. There is interest in reducing low frequency noise in several electronic devices such as Josephson junctionsand sigma-delta modulators[9–11] and the strategy outlined in this work could also potentially be used to reduce low frequency noise in these and other excitable systems such as lasers.

ACKNOWLEDGMENTS

This work was supported by the Canadian Institutes of Health Research (M.J.C, A.L., L.M.), the National Science and Engineering Research Council (M.J.C., A.L.), an Ontario Premier Research Award (A.L.), and the National Institutes of Health (J.B.).

REFERENCES

1. F. Rieke, D. Warland, R. R. de Ruyter van Steveninck, and W. Bialek, *Spikes: Exploring the Neural Code*, MIT Press, Cambridge, MA, 1996.
2. Z. F. Mainen, and T. J. Sejnowski, "Reliability of spike timing in neocortical neurons," *Science* **268**, pp. 1503–1506, 1995.
3. E. C. Cherry, "Some experiments on the recognition of speech, with one and two ears," *J. Accoust. Soc. Am.* **25**, pp. 975–979, 1953.
4. H. E. Derksen, and A. A. Verveen, "Fluctuations of Resting Neural Membrane Potential," *Science* **151**, pp. 1388–1392, 1966.
5. A. Destexhe, M. Rudolph, and D. Paré, " The high-conductance state of neocortical neurons *in vivo*," *Nat. Rev. Neurosci.* **4**, pp. 739–751, 2003.
6. J. Levin, and J. P. Miller, "Stochastic resonance enhances neural encoding of broadband stimuli in the cricket cercal sensory system," *Nature* **380**, pp. 165–168, 1996.
7. I. Goychuk, "Information Transfer with rate-modulated Poisson processes: A simple model for nonstationary stochastic resonance," *Phys. Rev. E* **64**, p. 021909, 2001.
8. N. J. Stocks, "Suprathreshold stochastic resonance in multilevel threshold systems," *Phys. Rev. Lett.* **84**, pp. 2310–2313, 2000.
9. S. R. Norsworthy, R. Schreier, and G. C. Temes, eds. *Delta-Sigma Data Converters*, IEEE Press, Piscataway, NJ, 1997.
10. A. M. Yacomotti, M. C. Eguia, J. Aliaga, O. E. Martinez, and G. B. Mindlin, "Interspike TIme Distribution in Noise Driven Excitable Systems," *Phys. Rev. Lett.* **83**, pp. 292–295, 1999.
11. K. Wiesenfeld, and I. Satija, "Noise Tolerance of frequency-locked dynamics," *Phys. Rev. B* **36**, pp. 2483–2492, 1987.
12. J. Shin, "Novel neural circuits based on stochastic pulse coding noise feedback pulse coding," *Int. J. Elec.* **74**, pp. 359–368, 1993.
13. J. Shin, "Adaptation in spiking neurons based on the noise shaping neural coding hypothesis," *Neural Networks* **14**, pp. 907–919, 2004.
14. D. J. Mar, C. C. Chow, W. Gerstner, R. W. Adams, and J. J. Collins, "Noise Shaping in populations of coupled model neurons," *Proc. Natl. Acad. Sci.* **96**, pp. 10450–10455, 1999.
15. W. R. Klemm, and C. J. Sherry, "Serial ordering in spike trains: what's it "trying to tell us"?," *Int. J. Neurosci.* **14**, pp. 15–33, 1981.

16. S. B. Lowen, and M. C. Teich, "Auditory-nerve action potentials form a nonrenewal point process over short as well as long time scales," *J. Accoust. Soc. Am.* **92**, pp. 803–806, 1992.
17. M. A. Lebedev, and R. J. Nelson, "High-frequency vibratory sensitive neurons in monkey primate somatosensory cortex: entrained and nonentrained responses to vibration during the performance of vibratory-cued hand movements," *Exp. Brain Res.* **111**, pp. 313–325, 1996.
18. A. Longtin, and D. M. Racicot, "Spike Train patterning and forecastability," *Biosystems* **40**, pp. 111–118, 1997.
19. R. Ratnam, and M. E. Nelson, "Non-renewal statistics of electrosensory afferent spike trains: implications for the detection of weak sensory signals," *J. Neurosci.* **20**, pp. 6672–6683, 2000.
20. M. J. Chacron, A. Longtin, M. St-Hilaire, and L. Maler, " Suprathreshold stochastic firing dynamics with memory in P-type electroreceptors," *Phys. Rev. Lett.* **85**, pp. 1576–1579, 2000.
21. D. R. Cox, and P. A. W. Lewis, *The Statistical Analysis of Series of Events*, Methuen, London, 1966.
22. M. J. Chacron, B. Lindner, and A. Longtin, "Noise Shaping by Interval Correlations Increases Information Transfer," *Phys. Rev. Lett.* **92**, p. 080601, 2004.
23. M. J. Chacron, B. Lindner, and A. Longtin, "ISI Correlations and Information Transfer," *Fluct. Noise Lett.* **4**, pp. L195–L205, 2004.
24. B. Lindner, M. J. Chacron, and A. Longtin, "Integrate-and-fire neurons with threshold noise - a tractable model of how interspike interval correlations affect neuronal signal transmission," *submitted*.
25. R. W. Turner, L. Maler, and M. Burrows eds., "Electroreception and electrocommunication,", *J. Exp. Biol.* **202**, pp. 1167–1458, 1999.
26. M. E. Nelson, and M. A. MacIver, "Prey capture in the weakly electric fish Apteronotus leptorhynchus: sensory acquisition strategies and electrosensory consequences," *J. Exp. Biol.* **202**, pp. 1195–1203, 1999.
27. G. H. K. Zupanc, and L. Maler, "Evoked chirping in the weakly electric fish Apteronotus leptorhynchus: a quantitative biophysical analysis," *Can. J. Zool.* **71**, pp. 2301–2310, 1993.
28. H. Scheich, T. H. Bullock, and R. H. Hamstra, "Coding properties of two classes of afferent nerve fibers: high frequency electroreceptors in the electric fish, eigenmania," *J. Neurophysiol.* **36**, pp. 39–60, 1973.
29. H. H. Zakon, "The electroreceptive periphery," in *Electroreception*, T. H. Bullock, and W. Heiligenberg, eds., pp. 103–156, Wiley, New York, 1986.
30. J. Bastian, "Electrolocation I. How the electroreceptors of Apteronotus albifrons code for moving objects and other electrical stimuli," *J. Comp. Physiol.A* **144**, pp. 465–479, 1981.
31. Z. Xu, J. R. Payne, and M. E. Nelson, "Logarithmic time course of sensory adaptation in electrosensory afferent nerve fibers in a weakly electric fish," *J. Neurophysiol.* **76**, pp. 2020–2032, 1996.
32. J. Benda, A. Longtin, and L. Maler, "Spike-frequency adaptation separates transient communication signals from background oscillations," *J. Neurosci.* (in press).
33. S. Bahar, J. W. Kantelhardt, A. Neiman, H. H. A. Rego, D. F. Russell, L. Wilkens, A. Bunde, and F. Moss, "Long-range temporal anti-correlations in paddlefish electroreceptors," *Europhys. Lett.* **56**, pp. 454–460, 2001.
34. A. Neiman, and D. F. Russell, "Stochastic byperiodic oscillations in the electroreceptors of paddlefish," *Phys. Rev. Lett.* **86**, pp. 3443–3446, 2001.
35. H. C. Tuckwell, *Nonlinear and stochastic theories, First Edition*, Cambridge University Press, Cambridge, 1988.
36. C. D. Geisler, and J. M. Goldberg, "A stochastic model of the repetitive Activity of Neurons," *Biophys. J.* **6**, pp. 53–69, 1966.
37. A. Rescigno, R. B. Stein, R. L. Purple, and R. E. Popele, "A neuronal model for the discharge patterns produced by cyclic inputs," *Bull. Math. Biophys.* **32**, pp. 337–353, 1970.
38. J. P. Keener, F. C. Hoppensteadt, and J. Rinzel, "Integrate-and-fire model of nerve membrane response to oscillatory input," *SIAM J. Appl. Math.* **41**, pp. 816–823, 1981.
39. G. Gestri, H. A. K. Masterbroek, and W. H. Zaagman, "Stochastic constancy, variability and adaptation of spike generation: performance of a giant neuron in the visual system of the fly," *Biol. Cybern.* **38**, pp. 31–40, 1980.
40. F. Gabbiani, and C. Koch, "Coding of Time-Varying Signals in Spike Trains of Integrate-and-Fire Neurons with Random Threshold," *Neural Comp.* **8**, pp. 44–66, 1996.

41. R. Azouz, and C. M. Gray, "Cellular mechanisms contributing to response variability of cortical neurons in vivo," *J. Neurosci.* **19**, pp. 2209–2223, 1999.
42. M. J. Chacron, A. Longtin, and L. Maler, "Simple models of bursting and non-bursting electroreceptors," *Neurocomputing* **38**, pp. 129–139, 2001.
43. M. J. Chacron, A. Longtin, and L. Maler, "Negative interspike interval correlations increase the neuronal capacity for encoding time-varying stimuli," *J. Neurosci.* **21**, pp. 5328–5343, 2001.
44. M. J. Chacron, K. Pakdaman, and A. Longtin, "Interspike interval correlations, memory, adaptation, and refractoriness in a leaky integrate-and-fire model with threshold fatigue," *Neural Comp.* **15**, pp. 253–278, 2003.
45. A. Longtin, C. Laing, and M. J. Chacron, "Correlations and Memory in Neurodynamical systems," in *Long-Range Dependent Stochastic Processes*, G. Rangarajan, and M. Ding, eds., pp. 286–308, Springer, Berlin, 2003.
46. M. J. Chacron, A. Longtin, and L. Maler, "The effects of spontaneous activity, background noise, and the stimulus ensemble on information transfer in neurons," *Network* **14**, pp. 803–824, 2003.
47. M. J. Chacron, A. Longtin, and K. Pakdaman, "Chaotic Firing in the sinusoidally forced leaky integrate-and-fire model with threshold fatigue," *Physica D* **192**, pp. 138–160, 2004.
48. M. J. Chacron, A. Longtin, and L. Maler, "To Burst or not to Burst?," *J. Comp. Neurosci.* **17**, pp. 127–136, 2004.
49. M. E. Nelson, Z. Xu, and J. R. Payne, "Characterization and modeling of P-type electrosensory afferent responses to amplitude modulations in a wave-type electric fish," *J. Comp. Physiol. A* **181**, pp. 532–544, 1997.
50. T. Cover, and J. Thomas, *Elements of Information Theory*, Wiley, New York, 1991.
51. A. Borst, and F. Theunissen, "Information theory and neural coding," *Nat. Neurosci.* **2**, pp. 947–957, 1999.
52. A. V. Holden, *Models of the Stochastic Activity of Neurons*, Springer, Berlin, 1976.
53. H. Risken, *The Fokker-Planck Equation*, Springer, Berlin, 1996.
54. J. Bastian, M. J. Chacron, and L. Maler, "Receptive field organization determines pyramidal cell stimulus-encoding capability and spatial stimulus selectivity," *J. Neurosci.* **22**, pp. 4577–4590, 2002.
55. J. Bastian, M. J. Chacron, and L. Maler, "Plastic and non-plastic cells perform unique roles in a network capable of adaptive redundancy reduction," *Neuron* **41**, pp. 767–779, 2004.
56. M. J. Chacron, L. Maler, and J. Bastian, "Electroreceptor Neuron Dynamics Shape Information Transmission," *submitted*.
57. T. Mickus, H. Y. Jung, and N. Spruston, "Properties of slow cumulative sodium channel inactivation in rat hippocampal CA1 pyramidal neurons," *Biophys. J.* **76**, pp.- 846–860, 1999.
58. L. Y. Wang, L. Gan, I. D. Forsythe, and L. K. Kaczmarek, "Contribution of the Kv3.1 potassium channel to high-frequency firing in mouse auditory neurones," *J. Physiol. Lond.* **509**, pp. 183–194, 1998.
59. A. J. Rashid, R. J. Dunn, and R. W. Turner, "A prominent soma-dendritic distribution of Kv3.3 K+ channels in electrosensory and cerebellar neurons," *J. Comp. Neurol.* **441**, pp. 234–247, 2001.
60. D. V. Madison, and R. A. Nicoll, "Control of the repetitive discharge of rat CA 1 pyramidal neurones in vitro," *J. Physiol.* **354**, pp.- 319–331, 1984.
61. M. V. L. Bennett, and S. Obara, "Ionic Mechanisms and Pharmacology of Electroreceptors," in *Electroreception*, T. H. Bullock, and W. Heiligenberg, eds., pp. 157–181, Wiley, New York, 1986.
62. X. J. Wang, "Calcium coding and adaptive temporal computation in cortical pyramidal neurons," *J. Neurophysiol.* **79**, pp. 1549–1566, 1998.
63. Y. H. Liu, and X. J. Wang, "Spike Frequency adaptation of a generalized leaky integrate-and-fire neuron," *J. Comput. Neurosci.* **10**, pp. 25–45, 2001.
64. J. W. Middleton, M. J. Chacron, B. Lindner, and A. Longtin, "Firing Statistics of a neuron driven by long-range correlated noise," *Phys. Rev. E* **68**, p. 021920, 2003.
65. F. Gabbiani, W. Metzner, R. Wessel, and C. Koch, "From stimulus encoding to feature extraction in weakly electric fish," *Nature* **384**, pp. 564–567, 1996.
66. W. Metzner, C. Koch, R. Wessel, and F. Gabbiani, "Feature extraction by burst-like spike patterns in multiple sensory maps," *J. Neurosci.* **18**, pp. 2283–2300, 1998.

67. B. Doiron, M. J. Chacron, L. Maler, A. Longtin, and J. Bastian, "Inhibitory feedback required for network oscillatory responses to communication but not prey stimuli," *Nature* **421**, pp. 539–543, 2003.
68. M. J. Chacron, B. Doiron, L. Maler, A. Longtin, and J. Bastian, "Non-Classical Receptive Field Mediates Switch in a Sensory Neuron's Frequency Tuning," *Nature* **423**, pp. 77–81, 2003.